AD-A089 267 NAVAL RESEARCH LAB WASHINGTON DC F/G 20/5
HIGH-POWER PICOSECOND PHOTOLYSIS OF SIMPLE ORGANIC MOLECULAR GA--ETC(U)
SEP 80 B B CRAIG, W L FAUST, L S GOLDBERG

UNCLASSIFIED NL

1 OF 1
AD A089267

END
DATE FILMED
10-80
DTIC

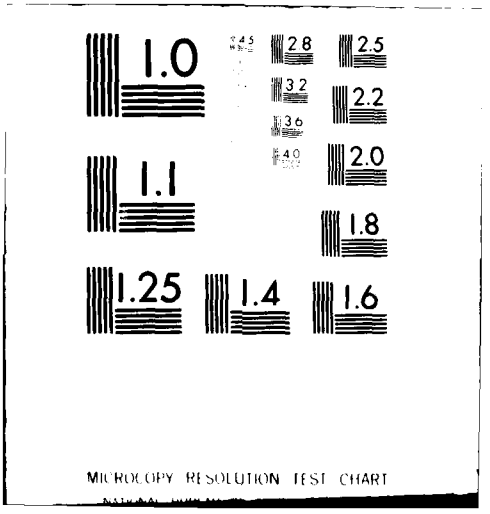
1.0
2.8
2.5
3.2
2.2
3.6
4.0
2.0
1.1
1.8
1.25
1.4
1.6
MICROCOPY RESOLUTION TEST CHART

HIGH-POWER PICOSECOND PHOTOLYSIS OF SIMPLE ORGANIC MOLECULAR GASES+

B.B. Craig*, W.L. Faust, L.S. Goldberg, J.M. Schnur,
P.E. Schoen and R.G. Weiss*

Naval Research Laboratory, Washington, D.C. 20375, U.S.A.
*Department of Chemistry, Georgetown University,
Washington, D.C. 20057, U.S.A.

ABSTRACT

High-power picosecond UV pulses from a Nd:YAG modelocked laser were used to induce a visible emission from a variety of gaseous organic molecules. We report the observation of electronically excited C_2, CH, CN and H fragments. The spectral characteristics and time development of the emitting species are highly dependent upon the structure of the parent molecules.

INTRODUCTION

Laser photolysis of simple molecules has contributed to a deeper understanding of dynamical processes in photodissociation. Our concern in the present work is with the decomposition of simple compounds which afford generic models of processes important in explosives, fuels and other energetic materials. Multiphoton IR and UV laser dissociation (1-4) has previously been applied to study the primary decomposition processes of gas-phase hydrocarbons and subsequent reaction of fragments having significance in the kinetics of combustion. These experiments have been performed in the nanosecond time domain and at millitorr gas pressures in order to maintain a collision-free time regime during the duration of the excitation pulse. In our experiments the time resolution afforded by picosecond pulse excitation enables such photolysis even at atmospheric pressures, yielding high fragment concentrations. For the pressures and high flux densities employed in this work, multiphoton absorption processes can be accompanied by dielectric breakdown (5). Indeed, since laser-induced breakdown is a nonresonant process, this very non-specificity facilitates the decomposition of a wide variety of materials.

Here, we demonstrate the utility of the technique in generating fragments whose emission spectra reflect their precursors. We have carried out the photolysis of ketene, methane, carbon monoxide and nitromethane at pressures in the range of 10-500 torr, and studied the luminescence from C_2, CH, CN and H fragments.

EXPERIMENTAL

Figure 1 shows a schematic of the Nd:YAG laser system. The flashlamp-pumped oscillator, operating at a 1 Hz repetition rate, employed a hybrid modelocking approach to provide more reproducible pulse-train generation. It utilized an active acousto-optic loss modulator (Quantronix) and a passive saturable absorbing dye (Eastman A9740) in a flow cell. The single 1064 nm pulse, switched from near the peak of the train, had ca. 0.4 mJ energy and typically 30 ps duration. Two stages of amplification, apodization and spatial filtering of the beam provided a high-spatial-quality IR pulse of 30-40 mJ energy. Efficient frequency doubling and redoubling in KD*P crystals generated a 4th harmonic (266 nm) photolyzing pulse of up to 10 mJ energy. The laser beam was focused to a 0.15 mm spot diameter in a static gas cell (ca. 100 cm^3) through a LiF window. The emitted light generated from individual laser shots was collected at right angles and focused into a grating monochromator coupled to a Nuclear Data ND100 intensified vidicon multichannel recording system (spectral sensitivity 380-800 nm). Improved signal-to-noise was achieved where necessary by accumulating data from typically 30 laser shots. High-resolution spectra were obtained with a Spex 0.8 m monochromator (0.1 nm system resolution). For time-resolved studies, a Varian VPM-154M cross-field photomultiplier was coupled to the exit slit of the monochromator. The transient signal was displayed on a Tektronix 7104 oscilloscope, giving a detection risetime of 400 ps. Observations were also made with an Electrophotonics streak camera (S-20 photocathode) having time resolution of 10 ps.

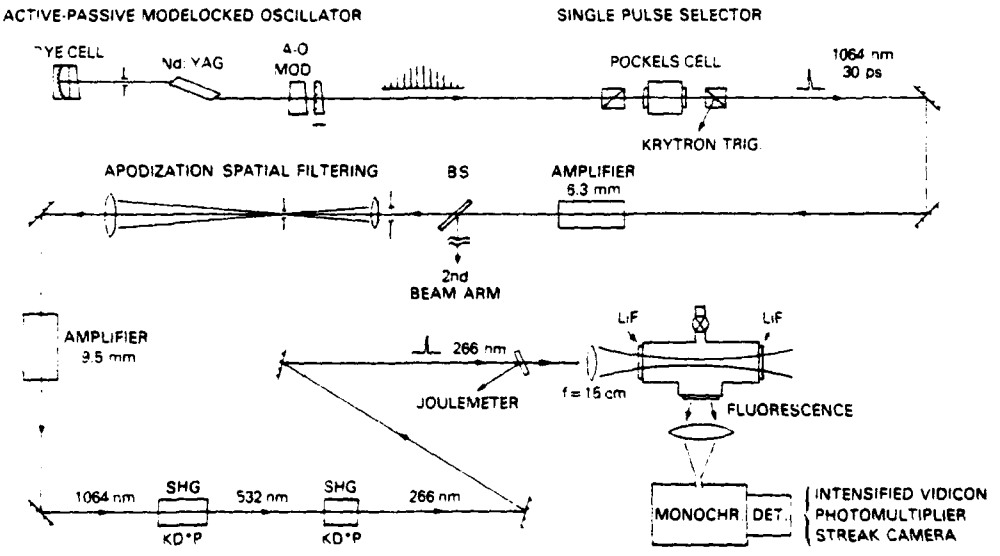

Fig. 1. Schematic of the laser system.

Methane was research grade purity supplied by Matheson Gas Products and was used without further purification. Carbon monoxide was ultra-high purity grade (Matheson) and was freed of any metal carbonyl contaminants by passing through a heated tube (200°C, atmospheric pressure) packed with glass wool (6). Nitromethane was Baker reagent grade and was distilled under nitrogen, collecting the middle fraction, b.p. 101-102°C. Ketene, CH_2CO, was prepared by a standard procedure (7) involving dehydration of acetic anhydride at 500-550°C and was purified by trap-to-trap distillation. It was stored in the dark under vacuum in a liquid nitrogen bath. A salt-ice bath placed between the reservoir and sample cell was used to condense traces of acetic acid and other high-boiling impurities.

RESULTS AND DISCUSSION

High-power, 30 ps pulses at 266 nm focused into the vapors under study (10-500 torr) generated a visible streak near the focal region. Low- and high-resolution spectra of the luminescence exhibited no differences in intensity or spectral distribution during a typical experiment involving several hundred laser shots. This indicates that stable photolytic products do not significantly affect the primary decomposition processes. The result is not surprising since the photolysed region is at least 10^6 smaller than the total sample volume. It should be emphasized that our analytical techniques give evidence only of luminescent species; other intermediates are undoubtedly produced.

Figure 2 depicts the similarity of the low-resolution emission spectra from ketene and carbon monoxide, each at 100 torr. High-resolution spectra indicate that the predominant emission belongs to the C_2 diradical in its triplet $d\,^3\Pi_g \rightarrow a\,^3\Pi_u$ Swan transition (8). Figures 3 and 4 show the $\Delta v = 0$ and $\Delta v = -1$ transitions for C_2 from carbon monoxide, methane and ketene. The emission spectra from methane and ketene exhibit a strong attendant rotational structure. In addition, a weak, underlying continuum emission, associated with a plasma formation, extended throughout the visible region. The intensity of this background varied for each gas studied but was most prominent for methane.

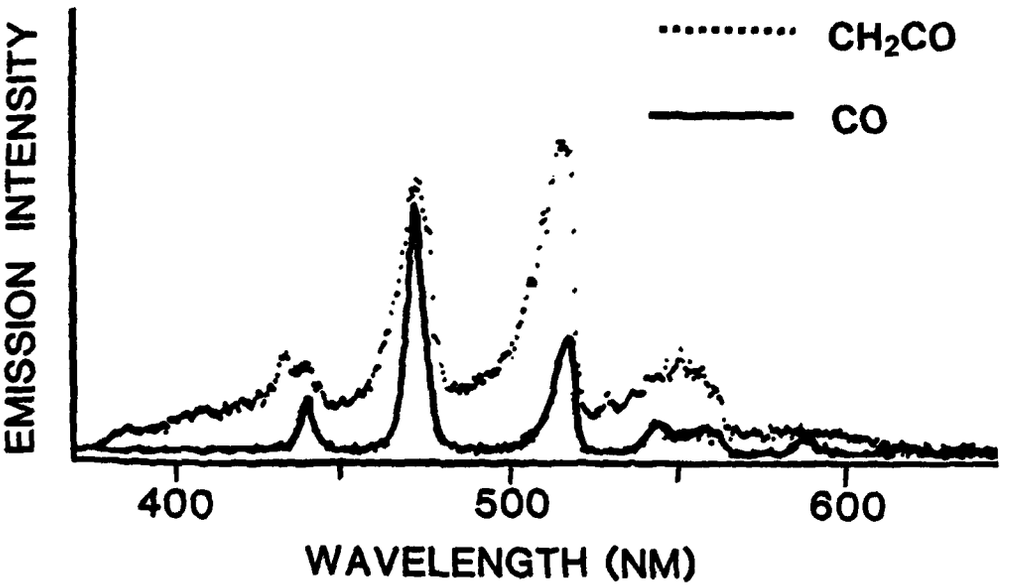

Fig. 2. Low-resolution (2 nm) emission spectra obtained when ketene and carbon monoxide, at 100 torr, are irradicated with individual laser pulses at 266 nm.

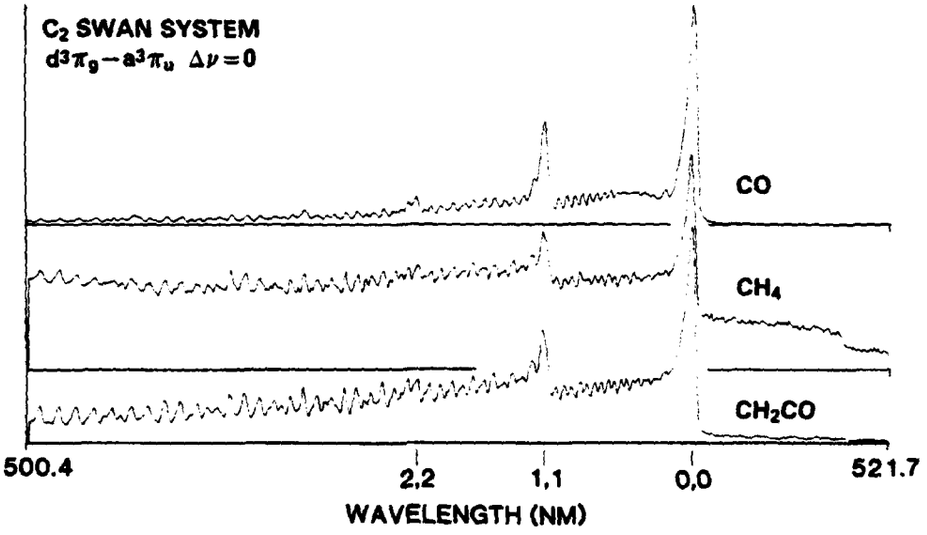

Fig. 3. High-resolution (0.1 nm) spectra of the Swan system emission ($\Delta v = 0$) derived from 266 nm irradiation of carbon monoxide, methane, and ketene, at 100 torr. Data are accumulated from 30 laser shots. Note the strong rotational decoration, to the high-energy side of the band heads, for methane and ketene.

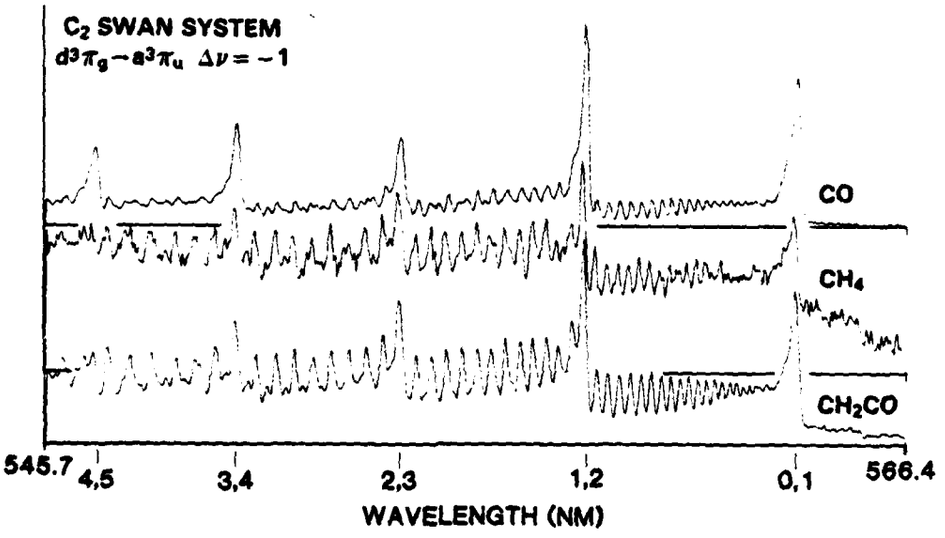

Fig. 4. Spectra of the Swan system emission ($\Delta v = -1$). Conditions as in Fig. 3

Figures 5 and 6 compare the regions of Swan $\Delta v = +1$ and $\Delta v = +2$ emission from carbon monoxide and ketene. Striking dissimilarities are evident at this resolution. Only in the case of CO are the C_2 "high-pressure" bands (9) observed. These are a consequence of the selective population of an upper vibrational level (generally attributed to $v' = 6$) (9) of the $d^3\Pi_g$ state and necessitate distinct formation mechanisms for the $^8C_2$ produced from carbon monoxide and ketene.

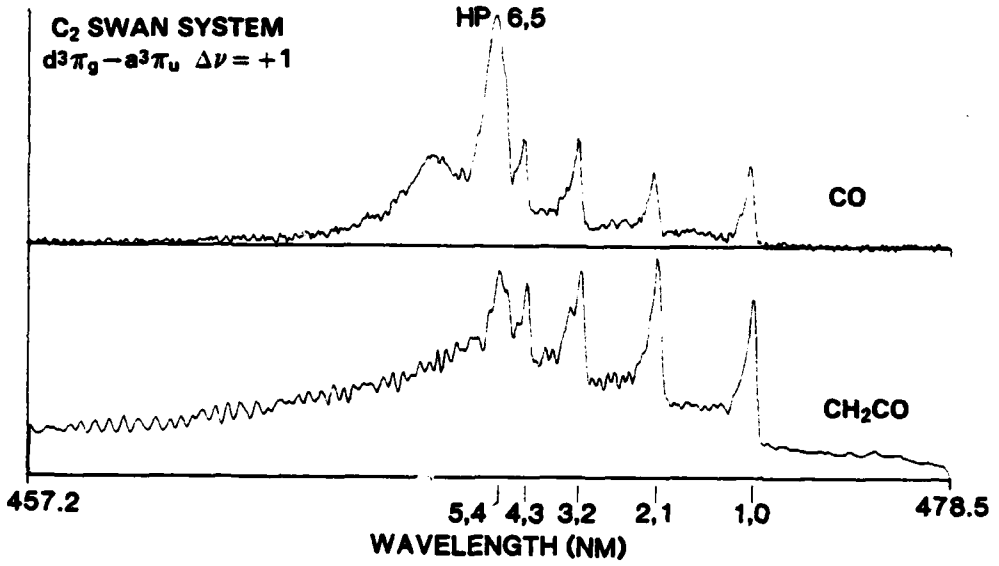

Fig. 5. Spectra of the Swan system emission ($\Delta v = +1$) derived from carbon monoxide and ketene, at 100 torr. Data are accumulated from 30 laser shots. The spectrum from CO also shows the high-pressure 6,5 band.

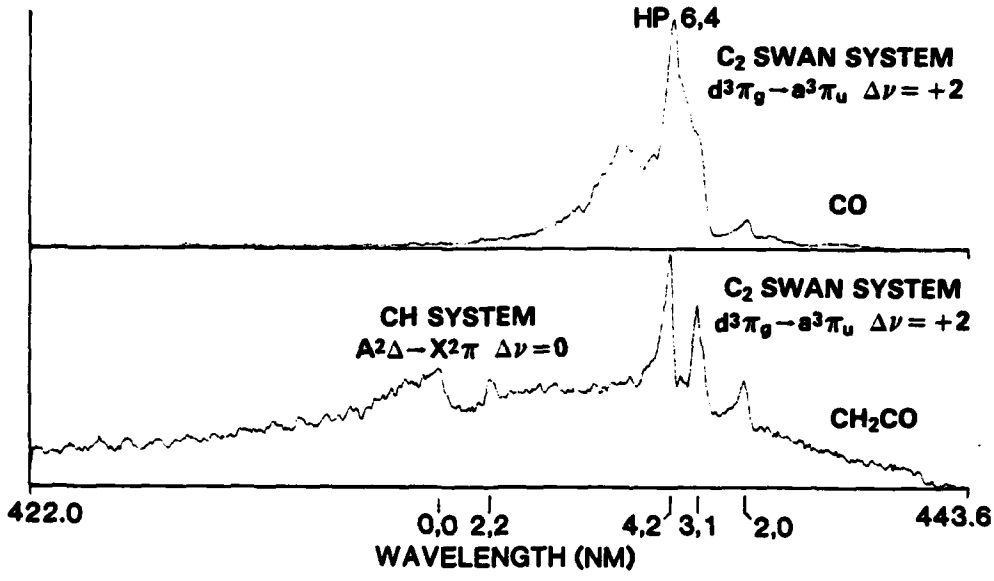

Fig. 6. Spectra of the Swan system emission (Δv = +2). Conditions as in Fig. 5. The spectra also show the high-pressure 6,4 band and CH emissions.

This difference of mechanisms finds further expression in the time-dependent oscilloscope data shown in Fig. 7. Figure 7A shows the risetime-limited formation of the $d^3\Pi_g$ emissive state (at 516 nm) of C_2 derived from ketene. The risetime is indistinguishable from that of the plasma radiation (upper trace), monitored at 616 nm where Swan emission is negligible. By contrast, no prompt C_2 emission is seen from CO (Fig. 7B) when either the normal or the high-pressure Swan bands are monitored. The oscillogram in Fig. 7B shows only the brief plasma emission, which can be detected throughout the visible region. Over much longer timescales (Fig. 7D), the slow, collisional formation of the $d^3\Pi_g$ state is observed. An intermolecular pathway leading to the formation of C_2, like that suggested by Kunz et al (10) (see Eqn. (1) and (2)), is consistent with these data:

$$C + CO + M \rightarrow C_2O + M \qquad (1)$$

$$C_2O + C \rightarrow C_2^* + CO \qquad (2)$$

M represents a third body and * refers to an unspecified electronic state of C_2. The highly-specific vibrational population of the

excited state is then rationalized as follows: there is a relaxation of the initial C_2 state to $b\,^3\Sigma_g^-$ which crosses $d\,^3\Pi_g$ near its sixth vibrational level (11). It has generally been accepted that the high-pressure emission orginates from $v' = 6$. However, the high-pressure bands lie to the low energy side of the corresponding normal Swan band head, where there are no rotational term differences. For example, the designated 6,5 high-pressure transition is at 468.0 nm while the regular 6,5 Swan band is observed at 466.9 nm (8,12). On this basis, we infer that the exact crossing between the $b\,^3\Sigma_g^-$ must occur below $v' = 6$.

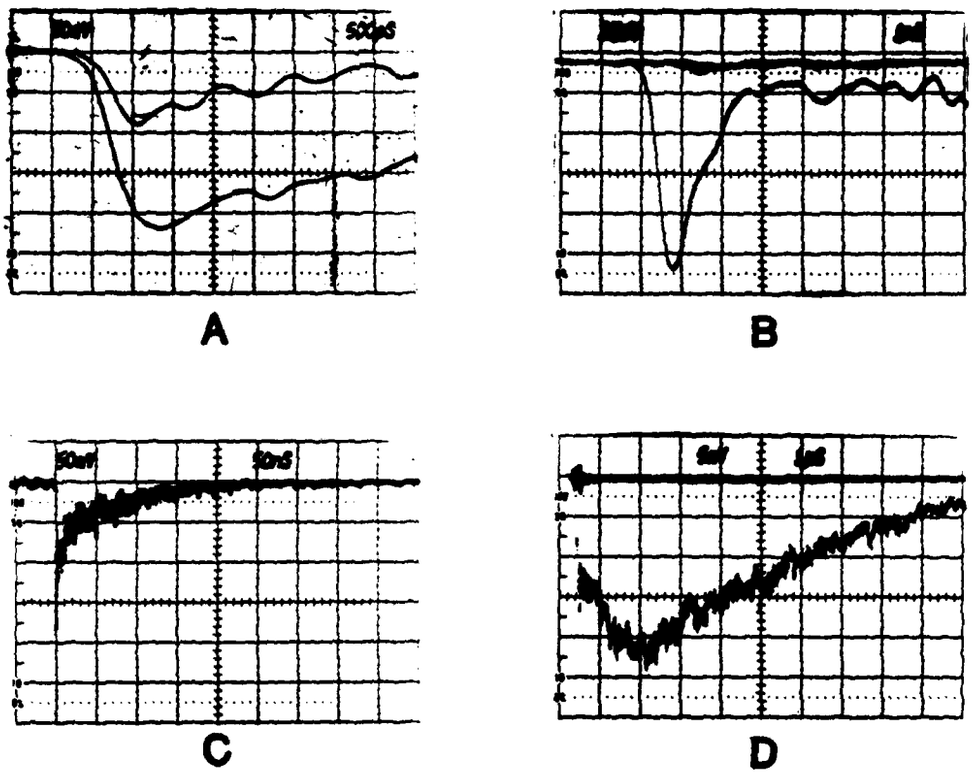

Fig. 7. Oscilloscope traces of the C_2 Swan emission monitored at 516 nm (0,0 transition). A: ketene, 100 torr, 500 ps/div. The upper trace shows the plasma radiation at 616 nm and should be reduced by a factor of 2.5 for comparison with the lower trace of C_2 emission. B: CO, 100 torr, 1 ns/div. C: ketene, 100 torr, 50 ns/div. D: CO, 100 torr, 1 μs/div.

Since the $d^3\Pi_g$ state collision-free lifetime has been determined as ca. 120 ns (3), it is clear that the slower decay in Fig. 7D does not reflect the kinetics of the $d^3\Pi_g \rightarrow a^3\Pi_u$ transition. Evidently we are following the formation and decay steps of an intermediate (consistent with Eqn. (1) and (2)), which become the rate-determining processes for the C_2 $d^3\Pi_g$ emission. Figure 7C indicates that the C_2 $d^3\Pi_g$ state has a lifetime of ca. 70 ns when produced in 100 torr of ketene. It is likely that the parent molecule and/or other photolysis fragments are involved in quenching steps. For instance, all the hydrogen bearing gases exhibit a strong pressure-broadened emission line at 656.3 nm, assigned to the Balmer Hα line of atomic hydrogen (Fig. 8).

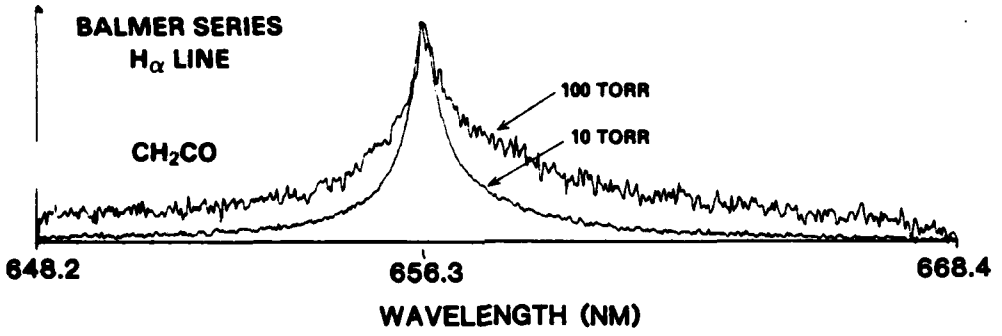

Fig. 8. Spectra of the atomic hydrogen Hα emission line derived from 266 nm irradiation of ketene. Note the strong pressure-broadening effect.

Returning to Fig. 7A, the C_2 derived from ketene appears with detection-system risetime (as noted in the caption, the contribution of the plasma to the lower trace is minimal). Such prompt C_2 formation suggests a unimolecular mechanism. However, a rapid collisional formation may be envisaged if the reacting fragments are created with substantial kinetic energy. Attempts to observe the formation using a streak camera have proved inconclusive. The spectral resolution required to minimize the prompt background has not allowed sufficient signal to be detected from the C_2 emission. In the case of methane, where C_2 production must be a collisional process, we have nonetheless been unable to follow it kinetically. The plasma radiation dominates the transient signal at 100 torr of methane for several nanoseconds, by which time the C_2 signal is fully developed.

The C_2 emission from methane and ketene show considerable rotational excitation, which implies a non-thermally-equilibrated population of excited C_2 molecules. C_2 emission spectra showing such abnormal rotation are ubiquitous in discharge (13) and laser photolysis (3) studies of simple organic molecules. In an intermolecular mechanism, "off-axis" collisions between fragments would be expected to impart excess rotation to a C_2 product. It is also possible that ketene undergoes unimolecular elimination of hydrogen and oxygen via out-of-plane bending motions, leaving C_2 with rotation. In the case of CO, the C_2 high-pressure system is obtained together with the normal Swan system, both showing the same protracted time development. This now gives temporal as well as spectral inference that C_2 is formed from CO by processes entirely distinct from those in ketene and methane. Consequently, it is not surprising that the emission spectrum exhibits much less rotational fine structure than that derived from ketene and methane.

Weak lines were observed at 410.2 nm and 406.8 nm only when ketene was photolysed. They are attributed to the Deslandres-d'Azambuja singlet C_2 system ($C^1\Pi_g \rightarrow A^1\Pi_u$, $\Delta v = -1$) (8). A weak flourescence at 431.4 nm (Fig. 6), observed for ketene and methane is attributed to CH emission ($A^2\Delta \rightarrow X^2\Pi$, $\Delta v = 0$) (8).

The power dependence of the C_2 emission is displayed in Fig. 9. At high input pulse energies, both carbon monoxide and ketene (100 torr) show a near-linear power dependence indicative of a saturation regime. The high-order nature of the excitation process is clearly evident from the steepening of the curves towards lower input energies. Furthermore, focusing of the excitation beam was essential for producing observable emission. Carbon monoxide and methane showed no emission at pressures below 10 torr. Ketene, however, which possesses a single-photon transition at 266 nm ($\varepsilon \approx 0.5$ mol^{-1} cm^{-1}) (14), exhibited luminescence even at pressures below 1 torr. The streak of visible emission extended somewhat beyond the focal region and had a more diffuse appearance than that observed at higher pressures. The excitation processes may well be different at lower pressures, but the observed luminescent products appear the same.

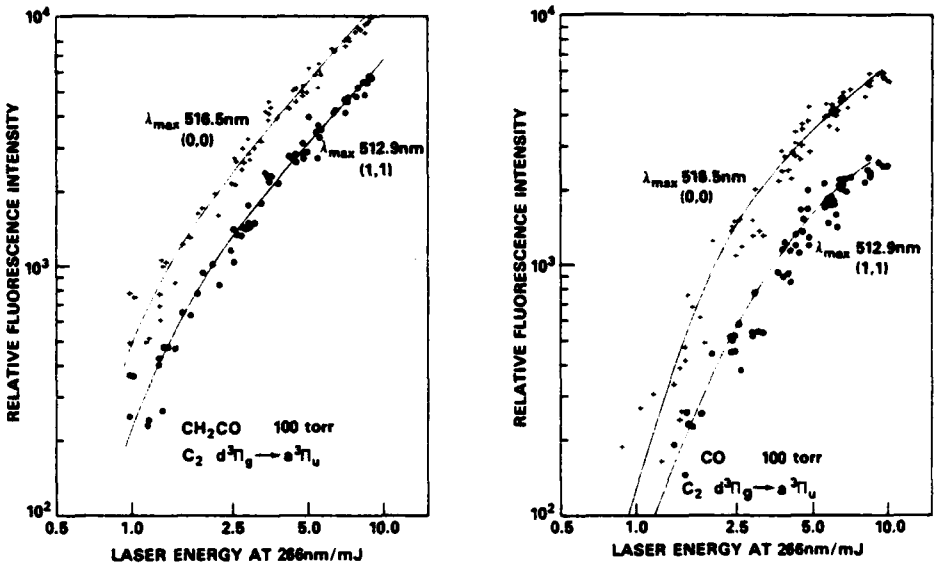

Fig. 9. Dependence of the C_2 Swan emission intensity on input laser pulse energy at 266 nm, from ketene (left) and carbon monoxide (right), at 100 torr.

Figure 10 compares the $\Delta v = 0$ C_2 Swan system observed from 15 torr of nitromethane with that from 10 torr of ketene. The C_2 band is substantially weaker in the case of nitromethane. It shows excess rotational excitation, as for ketene and methane. Furthermore, two new strong emissions were observed with bands heads at 421.6 nm and 388.3 nm (Fig. 10, below). These are assigned to the violet system of CN and arise from $B^2\Sigma^+ \rightarrow X^2\Sigma^+$ transitions (8). The $\Delta v = 0$ transition was also weakly observed in the case of ketene and carbon monoxide, indicating a slight nitrogen impurity.

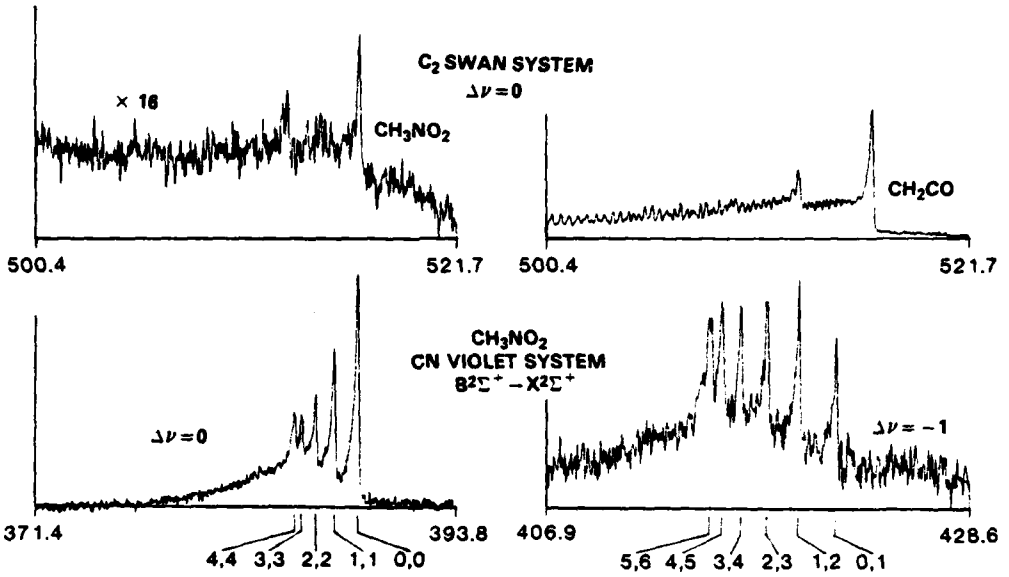

Fig. 10. Above: Spectra of the C_2 Swan emission ($\Delta v = 0$) derived from ketene at 10 torr and nitromethane at 15 torr. Note the reduced intensity of the signal from nitromethane. Below: Spectra of the CN violet system emission ($\Delta v = 0$, $\Delta v = -1$) derived from nitromethane at 15 torr. Data are accumulated from 30 laser shots.

The appearance of the strong CN emission from nitromethane and corresponding decrease in the C_2 emission might indicate that even under these harsh excitation conditions, the C-N bond remains intact. On the other hand, observations from conventional photolysis have been interpreted to support the scission of the C-N bond as the main primary process (15). The CN fragment from nitromethane could be generated unimolecularly, whereas by necessity C_2 is produced collisionally. Experiments are now in progress to follow the time development of the CN emission. In addition, we are examining other nitro-bearing alkanes which could provide an intramolecular C_2 formation pathway as a competing process with CN production.

SUMMARY

In this work we have extended to the picosecond realm the time definition for laser initiation and interrogation of gas-phase molecular dissociation, with spectral resolution adequate to isolate individual fragment species and indeed to observe rotational structure. We have examined the spectral and temporal characteristics of the dominant emitting fragments, C_2, CH, CN and H, observed in intense picosecond UV irradiation of ketene, methane, carbon monoxide and nitromethane. The rapid production of the C_2 $d^3\Pi_g$ state from methane and ketene (limited by the detection system risetime) suggests a similar mechanism of collisional formation, although a unimolecular process can not be ruled out in the case of ketene. Photolysis of CO also yields the C_2 $d^3\Pi_g$ state, which develops and decays collisionally over several microseconds. Its spectrum exhibits the high-pressure bands and shows much less rotational excitation than that obtained from ketene and methane. It is indicated that a rotationally nonthermalised C_2 $d^3\Pi_g$ population can be anticipated from precursors bearing CH_x. For nitromethane, time-resolved studies of the weak C_2 signal and accompanying CN emission should give some insight into the possible dissociative pathways. Future application of this technique to nitro-bearing alkanes and other related compounds may provide important information on reactions through which these molecules communicate in the early phases of rapid decomposition.

REFERENCES

+ Research supported in part by the Office of Naval Research and the Defense Advanced Research Projects Agency.

1. Chekalin, N.V., Dolzhikov, V.S., Letokhov, V.S., Lokhman, V.N., and Shibanov, A.N.: 1977, Appl. Phys. 12, pp 191-195.

2. Lesiecki, M.L., and Guillory, W.A.: 1977, J. Chem. Phys. 66, pp 4317-4324.

3. McDonald, J.R., Baronavski, A.P., and Donnelly, V.M.: 1978, Chem, Phys. 33, pp 161-170.

4. Filseth, S.V., Hancock, G., Fournier, J., and Meier, K.: 1979, Chem. Phys. Lett. 61, pp 288-292.

5. Ronn, A.M.: 1976, Chem. Phys. Lett. 42, pp 202-204.

6. Braker, W., and Mossmann, A.L.: 1971, Matheson Gas Data Book.

7. Nutall, R.L., Laufer, A.H., and Kilday, M.V.: 1971, J. Chem. Thermodyn. 4, pp 167-174.

8. Pearse, R.W.B., and Gaydon, A.G.: 1965, Identification of Molecular Spectra, Chapman and Hall, London.

9. Herzberg, G.: 1946, Phys. Rev. 70, pp 762-764.

10. Kunz, C., Harteck, P., and Dondes, S.: 1967, J. Chem. Phys. 46, pp 4157-4158.

11. Read, S.M., and Vanderslice, J.T.: 1962, J. Chem. Phys. 36, pp 2366-2369.

12. Johnson, R.C.: 1927, Phil. Trans. Royal Soc. A. 266, pp 157-230.

13. Lochte-Holtgreven, W.: 1930, Z. für Physik. 64, pp 443-451.

14. Laufer, A.H., and Keller, R.A.: 1971, J. Am. Chem. Soc. 93, pp 61-63.

15. Honda, K., Mikuni, H., and Takahasi, M.: 1972, Bull. Chem. Soc. Japan.: 45, pp 3534-3541.